Program Digest, 2019 IEEE International Ultrasonics Symposium (IUS)
Glasgow, Scotland, October 6-9, 2019

Self-propelled Swimmer Propulsion System using SAW and BAW

Kazuki Nishio
Tokyo Institute of Technology
Yokohama, Japan
nishio.k.af@m.titech.ac.jp

Deqing Kong
Tokyo Institute of Technology
Yokohama, Japan
kong.d.aa@m.titech.ac.jp

Minoru Kuribayashi Kurosawa
Tokyo Institute of Technology
Yokohama, Japan
mkur@ip.titech.ac.jp

***Abstract*—Many researches on self-propelled swimmer actuators using ultrasonic vibrators have been discussed with acoustic streaming. However we suggest that this is due to the acoustic radiation force caused by the acoustic impedance difference. In this research, we make two kinds of swimmers using surface acoustic wave (SAW) that generates 9.6MHz Rayleigh wave and bulk acoustic wave (BAW) that generates 1.6MHz Bulk wave, and compare the thrust of swimmers calculated acoustic radiation force from vibration velocity and measure using digital force gauge. The results show that the order of thrusts of SAW and BAW are much different. The movement of the interface between the ultrasonic transducer and the liquid is required to discuss more strictly.**

Keywords—SAW; BAW; microrobot; swimmer; drug carrier; acoustic microfluidics; actuator; interdigital transducer

I. Introduction

Recently, several submerged actuators that have been studied for diverting to microrobots have been announced [1-6]. However, these actuators require external operation or are complicated and difficult to miniaturize. In addition, there are concerns about malfunctions and performance degradation due to the effects of adhesion of blood components and impurities in the fluid.

Research on swimmer actuators using ultrasonic transducers is spreading to solve the problem [7-10]. Some current research uses PZT transducers that vibrate thickness to generate bulk waves. In these studies, the generation of thrust is a phenomenon caused by acoustic streaming. To our knowledge, because the force from acoustic streaming does not work directly on the swimmer, the swimmer is moving with other forces. In this study, we have proposed a self-propelled swimmer actuator with a different mechanism using Rayleigh waves, which are surface acoustic waves, and suggest that thrust generation by ultrasonic transducers is a phenomenon based on acoustic radiation force theory during the research process [11,12]. In this research, two kinds of swimmers were designed using SAW that generates 9.6MHz Rayleigh wave and BAW that generates 1.6MHz bulk wave, and compared the thrust of swimmers calculated acoustic radiation force from vibration velocity and measured using a digital force gauge.

II. Propulsion Principle

A. Acoustic Radiation Force

Radiation pressure P_{ac} acting on the object in the sound field is calculated as the acoustic energy density obtained by time-averaged incident plane sound waves as $\langle E_i \rangle$ [13].

As shown in Fig.1, it is assumed that media with different specific acoustic impedances ($z_1 = \rho_1 c_1, z_2 = \rho_2 c_2$ where ρ_1 and ρ_2 are densities and c_1 and c_2 are sound velocities) are in contact with the boundary plane at $x = 0$. A portion of the acoustic energy of the incident wave is reflected to $-x$ side and the rest is transmitted to $+x$ side due to the reflectance and transmittance determined by the ratio of the specific acoustic

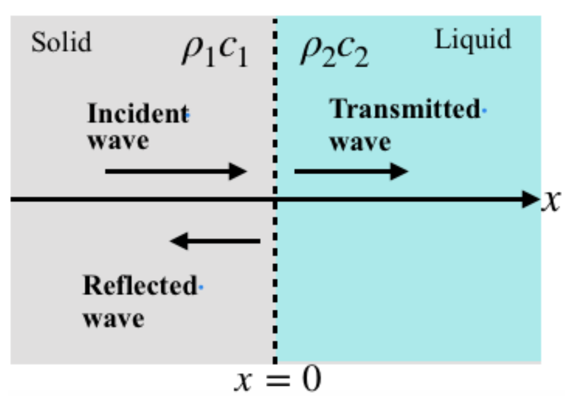

Fig. 1 Coordinate system of acoustic radiation force

impedance. As a result, the acoustic energy density at the boundary surface difference occurs, and a pressure difference occurs in the direction in which the difference decreases. This is radiation pressure.

Considering the case where a plane wave of time-average acoustic energy density $\langle E_i \rangle$ is perpendicularly incident in $+x$ direction on the boundary surface At this time, the time-average acoustic energy density $\langle E \rangle$ in space is

$$\langle E \rangle = \begin{cases} (1+R_P^2) \ \ \langle E_i \rangle & (x<0) \\ \frac{c_1}{c_2} Z T_P^2 \ \ \langle E_i \rangle & (x>0) \end{cases} \tag{1}$$

where, $Z = z_1/z_2$ and the acoustic reflectivity is $R_P = (1-Z)/(1+Z)$, the sound pressure transmittance is $T_P = 2/(1+Z)$. When the sound pressure amplitude of the incident wave is P_0, the time average acoustic energy density $\langle E_i \rangle$ is

$$\langle E_i \rangle = \frac{P_0^2}{2\rho_1 c_1^2} \tag{2}$$

Therefore, the interface receives $(1+R_P^2)\langle E_i \rangle$ pressure from $x<0$ side and $(c_1/c_2) Z T_P^2 \langle E_i \rangle$ pressure from $x>0$ side. The difference is showed

$$P_{ac} = \frac{2}{(1+Z)^2}\left(1+Z^2-2Z\frac{c_1}{c_2}\right)\langle E_i \rangle \tag{3}$$

and this equation means acoustic radiation pressure. The sound pressure amplitude is

$$P_0 = 2\pi f A \rho_1 c_1 \tag{4}$$

based on the vibration velocity consisting of vibration amplitude A and drive frequency f. The value obtained by multiplying the equation (3) by the area is the acoustic radiation force. From equations (2) and (4), it can be seen that the acoustic radiation force is proportional to the square of the vibration velocity.

B. Acoustic Radiation Force by SAW

Fig.2 shows how Rayleigh waves are radiated into water. SAW becomes leaky SAW (LSAW) while radiating longitudinal waves into water. When the propagation velocity in water is V_W and the propagation velocity in lithium niobite is V_R, the radiation angle (Rayleigh angle) θ_R is expressed as follows.

$$\theta_R = \sin^{-1}(V_W/V_R) \tag{5}$$

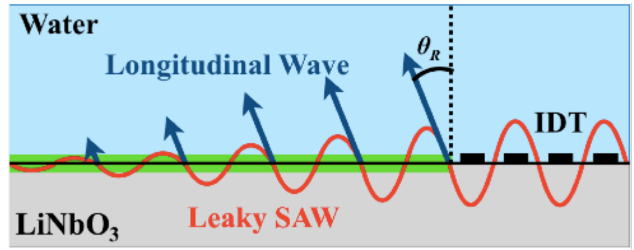

Fig. 2 Acoustic radiation into liquid by SAW.

Table 1 Characteristics of underwater SAW[14].

		SAW propagation speed (m/s)	LSAW propagation speed(m/s)	$\Delta x/\lambda$
128° y-rotated x-propagation lithium niobate	short	3882	$3884 + j70.7$	8.74
	open	3994	$3931 + j67.7$	9.24

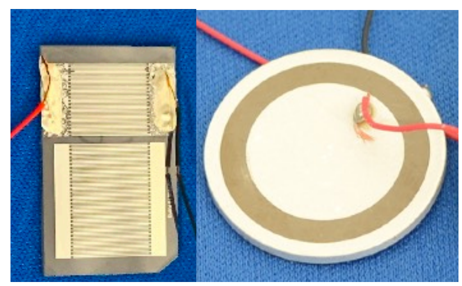

(a) SAW device (b) BAW device (20x1.0 mm)

Fig. 3 Ultrasonic transducers used in the experiment.

Propagation speed and attenuation are shown Table 1. Δx indicates the distance until the amplitude of the leaky surface acoustic wave attenuates to $1/e$, in units of wavelength λ. The actual value is $\theta_R = 22°$.

III. Experiment

A. SAW and BAW Devices

The SAW and BAW devices used are shown in Fig.3 (a) and (b) [15,16].The vibration amplitude was measured using a laser Doppler vibrometer. At this time, a device was placed on the bottom of the water tank and a laser beam was applied vertically from above the water surface. The SAW device has a feature that the vibration amplitude changes linearly with respect to the driving voltage. The point with the largest vibration amplitude was measured and was 6.3 nm at a drive voltage of 40 Vpp the whole surface. The BAW device was plotted in 0.5mm increments to measure the overall vibration distribution. However, the water surface could be greatly disturbed. Fig. 4 shows the vibration amplitude when the drive voltage is 3 Vpp. Density of water is $1.0\times10^{3}\ \mathrm{kg/m^{3}}$, sound propagation velocity is 1500 m/s. Density of 128° y-rotated x-propagation lithium niobate is $4.65\times10^{3}\ \mathrm{kg/m^{3}}$ and sound propagation velocity is 3994 m/s. Density of PZT is $7.65\times10^{3}\ \mathrm{kg/m^{3}}$ and sound propagation velocity is 4390 m/s. The effective area of SAW device is $26\mathrm{mm}\times9\mathrm{mm}$ for simplicity, and the effective area of the BAW device is in the range of radius 6.5mm in the center.

B. *Swimmer Actuator*

The SAW swimmer was designed so that the vibration direction of the ultrasonic wave radiated longitudinally was parallel to the water surface as shown in Fig.5 and Fig.6. In addition, as shown in Fig.7 and Fig.8, the BAW swimmer to sandwich an ultrasonic vibrator that vibrates in thickness between an air layer and a liquid layer so that the acoustic radiation force is greatly generated in one direction at the interface with the liquid was designed.

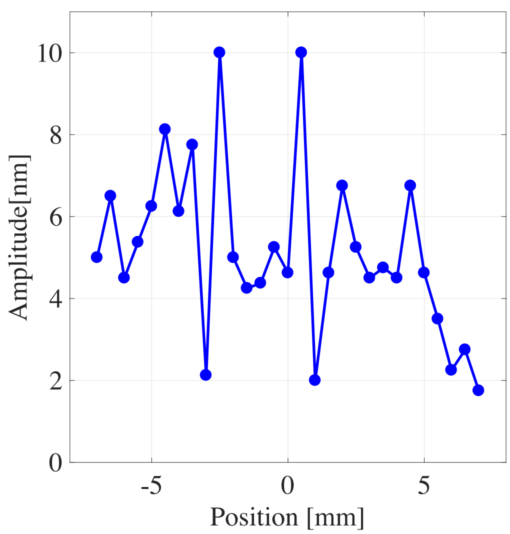

Fig. 4 Vibration distribution on a straight line of BAW when the drive voltage is 3Vpp.

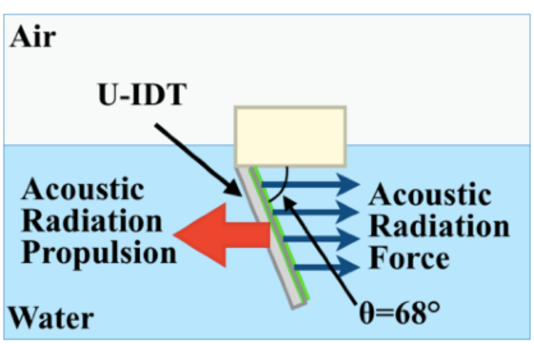

Fig. 5 Schematic view of SAW swimmer actuator.

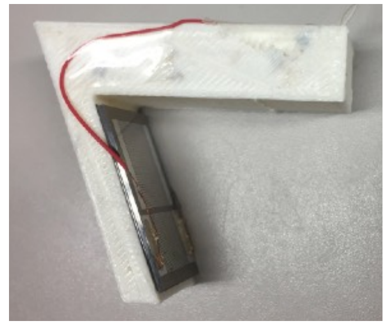

Fig. 6 Prototype of SAW swimmer actuator.

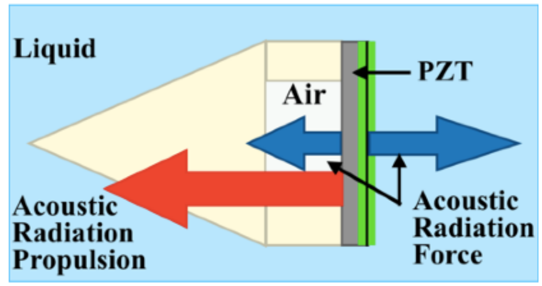

Fig. 7 Schematic view of BAW swimmer actuator.

Fig. 8 Prototype of BAW swimmer actuator.

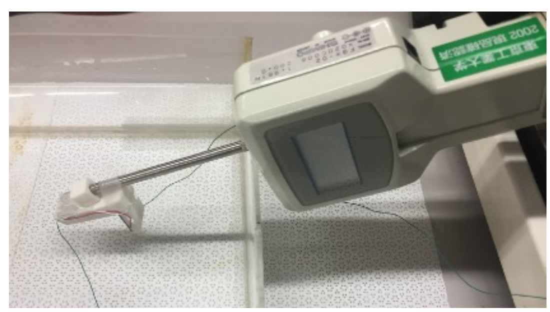

Fig. 9 Thrust measurement environment.

C. *Thrust Measurement*

Fig 9 shows the thrust measurement environment. By setting a swimmer actuator at the tip of the digital force gauge, it was set so that pure thrust can be measured.

The measurement results of SAW swimmer and BAW swimmer are shown in Fig. 10 and Fig. 11, respectively.The thrust of the SAW swimmer measured with a digital force gauge was 4 mN at 100 Vpp from Fig. 10, and 0.5 mN from

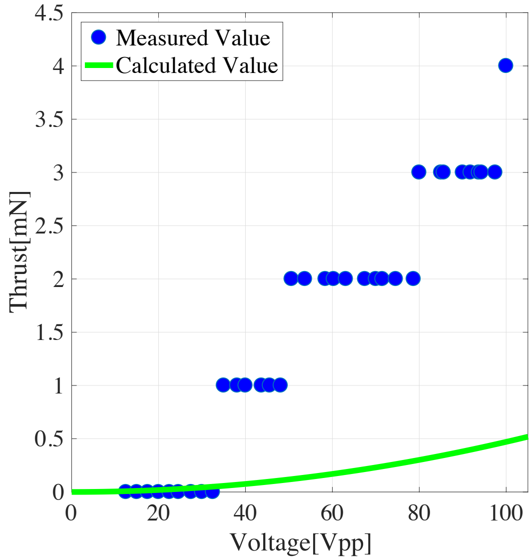

Fig. 10 No load thrusts of SAW swimmers by diverse voltages.

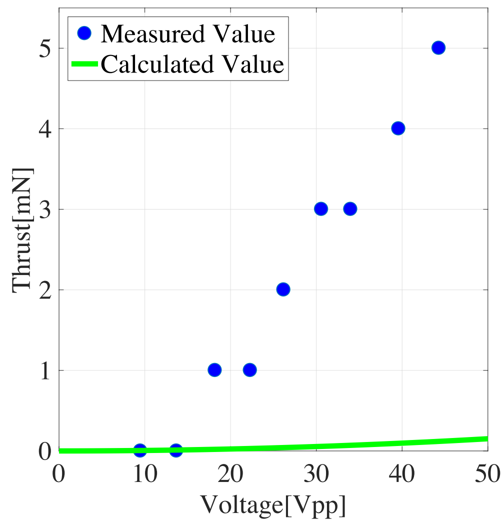

Fig. 11 No load thrusts of BAW swimmers by diverse voltages.

the calculation. And that of the BAW swimmer measured with a digital force gauge was 5mN from Fig. 11 to 44 Vpp, and 0.2 mN from the calculation. In both cases, the calculated value obtained from the equation (3) much different.

IV. Conclusion

It was shown that the propulsion principle of a swimmer actuator using an ultrasonic transducer is due to acoustic radiation force. However, the calculated value of thrust and the measured value did not completely coincide. In order to solve this problem, it is necessary to discuss the motion of the interface between the ultrasonic transducer and the liquid more precisely. It is also necessary to improve the measurement of vibration amplitude with a laser Doppler vibrometer in depth.

Acknowledgment

The authors wish to thank The Japan Keirin Association Foundation (JKA Foundation) and JSPS KAKENHI Grant Number JP19H02092 for providing the research funds of the novel swimmer actuator.

References

[1] Jinxing Li, Berta Esteban-Fernández de Ávila, Wei Gao, Liangfang Zhang, Joseph Wang, “Micro/nanorobots for biomedicine: Delivery, surgery, sensing, and detoxification,” Sci.Robot.2, eaam6431, 2017.

[2] Alexander A. Solovev, Yongfeng Mei, Esteban Bermu´ dez Uren˜ a, Gaoshan Huang, and Oliver G. Schmidt, “Catalytic Microtubular Jet Engines Self-Propelled by Accumulated Gas Bubbles,” small 2009, No. 14, 1688-1692, 5, 2009.

[3] Victor Garcia-Gradilla, Jahir Orozco, Sirilak Sattayasamitsathit, Fernando Soto, Filiz Kuralay, Ashley Pourazary, Adlai Katzenberg, Wei Gao, Yufeng Shen, and Joseph Wang, “Functionalized Ultrasound-Propelled Magnetically Guided Nanomotors: Toward Practical Biomedical Applications,” ACSNANO, Vlo.7, No.10, 9232-9240, 2013.

[4] Ambarish Ghosh and Peer Fischer, “Controlled Propulsion of Artificial Magnetic Nanostructured Propellers,” NANO LETTERS, Vol.9, No.6, pp.2243-2245, 2009.

[5] Bradley J Ioannis K. Kaliakatsos,and Jake J. Abbott, “Microrobots for Minimally Invasive Medicine,” Anna.Rev.Biomed.Eng, pp.55-85, 12, 2010.

[6] Veronika Magdanz Mariana Medina-Sánchez, Yan Chen, Maria Guix, and Oliver G. Schmidt, ”How to Improve Spermbot Performance,” Adv.Funky.Mater, 25, pp.2763-2770, 2015.

[7] E. M. Allison, George S. Springer, and Jacques Van Dam, "Ultrasonic propulsion," Journal of Propulsion and Power, vol. 24, pp.547-553, 2008.

[8] A.C.H.Tan and F.S.Hover, “Thrust and wake characterization in small, robust ultrasonic thrusters,” OCEANS 2010 MTS/IEEE SEATTLE, pp. 1-9, 2010.

[9] Hongyu Yu and Eun Sok Kim, “Ultrasonic underwater thruster”. IEEE International Micro Electro Mechanical Systems Conference, Maastricht, The Netherlands, pp.486-489, 2004.

[10] Yannyk Bourquin and Jonathan M Cooper, “Swimming Using Surface Acoustic Waves,” PLoS ONE, 8(2):e42686, Feb, 2013.

[11] Deqing Kong and M. K. Kurosawa, “A novel swimmer actuator via leaky surface acoustic wave,” IEEE International Ultrasonics Symposium, pp.1-4, 2018.

[12] Deqing Kong, Kazuki Nishio and M. K. Kurosawa, “A novel approach to swimmer actuation via leaky surface acoustic wave,” International Conference on Micro Electro Mechanical Systems, pp.994-997, 2019

[13] Tomoo Kamakura and Shigemi Saito, “Nonlinear Acoustics Fundamentals and Applications,” Corona Publishing Co, pp.156-194. 2014.

[14] Toyokawa Miriizumi, Takamichi Nakamoto and Tsuneo Kikuchi, “Selection of piezoelectric materials for interdigitated electrode underwater transducers,” IEICE, A. VolJ65-A, No.5, pp.489-490, 1982.

[15] D. Kong and M. K. Kurosawa, “Stator optimization and evaluation method in a surface acoustic wave motor,” Jpn. J. Appl. Phys. 54, pp. 07HB01(1-4), 2015.

[16] D. Kong and M. K. Kurosawa, “Excitation of Rayleigh wave with sapphire/$LiNbO_3$ mechanical integration for surface acoustic wave motor,” Jpn. J. Appl. Phys. 57, pp. 07LE07(1-5), 2018.